A new acid-processing route to polyaniline films which exhibit metallic conductivity and electrical transport strongly dependent upon intrachain molecular dynamics

1998 J. Phys.: Condens. Matter 10 8293

(http://iopscience.iop.org/0953-8984/10/37/015)

J. Phys.: Condens. Matter **10** (1998) 8293–8303. Printed in the UK PII: S0953-8984(98)92813-2

A new acid-processing route to polyaniline films which exhibit metallic conductivity and electrical transport strongly dependent upon intrachain molecular dynamics

P N Adams, P Devasagayam, S J Pomfret, L Abell and A P Monkman

Organic Electroactive Materials Research Group, Rochester Building, Physics Department, Durham University, South Road, Durham DH1 3LE, UK

Received 30 March 1998, in final form 18 May 1998

Abstract. Conductive polyaniline (PANi) films have been prepared via a new route comprising 2-acrylamido-2-methyl-1-propanesulphonic acid (AMPSA) as both the protonating acid and the solvating group, and dichloroacetic acid (DCA) as a solvent. The AMPSA content was varied so that between 30 and 100% of the nitrogen sites on polyaniline could be protonated. The temperature dependence of the conductivity of the films was measured between 15 and 300 K. Above 75–115 K, depending upon the protonation level, a negative temperature coefficient was observed. At 240–260 K a new transition was observed, essentially independent of the protonation level, above which the negative temperature dependency becomes much stronger. The conductivity data were fitted using a simple model employed previously for films of polyaniline camphorsulphonate, and comparisons made between the two systems.

Differential scanning calorimetry measurements on a series of films showed an endothermic transition centred at 240–254 K, whose magnitude is dependent upon the AMPSA content. This thermal transition is ascribed to increased motion in the AMPSA anions when heated to above the transition temperature. The AMPSA anion may be considered to behave as a side chain ionically bonded to the PANi backbone, whose particular structure will affect the intrachain molecular dynamics, and hence electrical transport properties of the bulk polymer. The observed thermal transition correlates well with the new transition seen in the conductivity data.

It was possible to draw films of PANi·$AMPSA_{0.6}$ uniaxially both at room temperature and at 363 K. The room temperature conductivity along the stretch direction was increased to a maximum value of 670 ± 55 S cm^{-1} for a film drawn at 363 K, compared to 210 ± 20 S cm^{-1} for an undrawn sample. The films are compared to previous results obtained with polyaniline films protonated with 10-camphorsulphonic acid (CSA).

1. Introduction

Since 1992, it has been possible to process the protonated (doped) form of polyaniline (PANi) into films [1] and fibres [2], using 10-camphorsulphonic acid (CSA) as a protonating/solvating group and m-cresol as a solvent. The conductivity showed a positive, then negative (non-metallic then metallic) temperature dependence, as the temperature was increased [3]. The 'turnover' temperature, or temperature at which the maximum conductivity occurs, can be as low as 135 K for PANi·$CSA_{0.6}$, i.e. polyaniline in which 60% of the nitrogens are protonated with camphorsulphonic acid [4]. It was also possible to align the polymer chains in these films by heating to 423 K while applying uniaxial stress. The maximum conductivity obtained by this method was 970 ± 30 S cm^{-1} along the stretch direction, measured at room temperature [5]. It was decided to find and study

0953-8984/98/378293+11$19.50

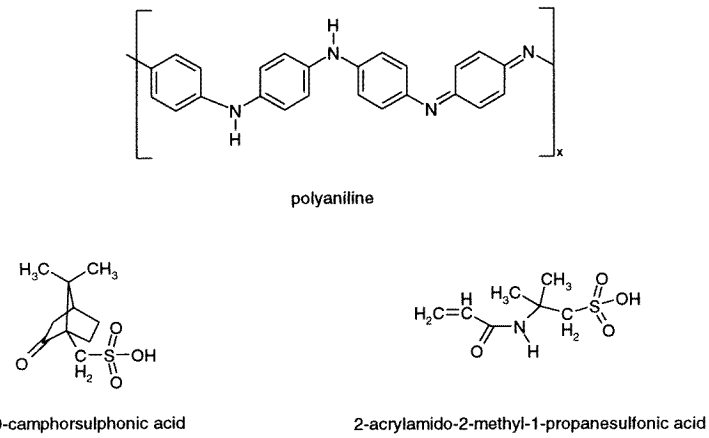

Figure 1. Structures for the emeraldine base form of polyaniline, 2-acrylamido-2-methyl-1-propanesulphonic acid and 10-camphorsulphonic acid.

alternatives to the CSA/m-cresol system which would have the possibility of showing both lower toxicity than the m-cresol and greater processibility by using a less bulky sulphonic acid.

Previous studies had already tried using different solvents for PANi·$CSA_{0.5}$ [6, 7], including dichloroacetic acid (DCA), which gave a film with a conductivity of 80 S cm^{-1} [6] at room temperature. Similarly, an amidopropanesulphonic acid had also been used as a dopant for spinning thin polyaniline films from solvents such as trifluoroethanol [8], to give a coating with a conductivity of 100 S cm^{-1}. In this paper, we present the results for the combination of polyaniline protonated with 2-acrylamido-2-methyl-1-propanesulphonic acid (AMPSA), and using DCA as a solvent. The solutions were readily processible, forming both solvent-cast films and fibres (the latter using higher-concentration solutions/dispersions and a coagulating solvent [9]), which could be drawn at room temperature or above. Differential scanning calorimetry (DSC) was used to search for any thermal transitions in the films which could account for this drawability. Measurements of the temperature dependence of the conductivity were performed on the films and compared to previous results obtained with polyaniline protonated with camphorsulphonic acid. The structures for the emeraldine base form of polyaniline, 10-camphorsulphonic acid and 2-acrylamido-2-methyl-1-propanesulphonic acid are shown in figure 1.

2. Experimental procedure

2.1. Sample preparation

High-molecular-weight polyaniline ($M_w \sim 2 \times 10^5$ g mol^{-1}), synthesized in Durham at 248 K [10, 11], was used as the starting material. AMPSA and DCA were obtained from Aldrich Chemicals and used without further purification or drying. The base form of the polyaniline was ground in a mortar and pestle with sufficient AMPSA to protonate between 30 and 100% of the nitrogens in polyaniline. Each sample was added to 20.0 g of DCA so that the total concentration for each sample was 1.5% w/w. Using an Ultraturrax T25 homogenizer, the samples were dissolved/dispersed by mixing at 20 000 rpm for 10 minutes,

then centrifuged at 4000 rpm for 30 minutes to remove any undissolved material, of which there was no visible sign. The dark green solutions were poured onto silicon wafers and dried in an oven at 353 K for 24 hours. The films were then peeled away from the silicon wafer and cut into thin strips. These were placed inside an evaporator and four-in-line parallel gold electrodes deposited under vacuum.

2.2. Conductivity/temperature measurements

The samples were placed in a closed-loop helium cryostat which utilized four platinum contact wires, spaced so that they overlapped the gold electrodes on the films. Conductivity measurements were made over the range of 15 to 300 K under a dynamic vacuum. A current of 500 μA was passed between the two outer Pt wires and the potential difference measured between the inner two Pt wires, using standard four-in-line geometry. The temperature was raised to 300 K in steps of 5 K, with conductivity measurements made every 20 minutes, the current only being applied during each measurement. The samples were found to obey Ohm's law over the current range employed.

2.3. Stretched films

A second solution comprising 0.90 g of PANi·AMPSA$_{0.6}$, homogenized in 44.10 g of DCA, was poured onto a 12.5 cm diameter silicon wafer and dried at 333 K. The resulting film was thicker than the previous examples, and a dumb-bell-shaped cutter was used for preparing samples for orienting under stress. Samples of film were heated to 363 K and the stress applied so that the films stretched at a rate of 0.05 cm s^{-1}. Films stretched to 120, 150 and 180% elongation, and an unstretched sample of the same film, were coated with gold electrodes and the conductivities measured between 15 and 300 K. Perpendicular-conductivity measurements on the sample stretched to 150% elongation were made by turning the film through 90° and depositing the four gold electrodes so that they ran parallel to the stretch direction. This sample measured 1.33 cm across the width of the film, whereas the other samples stretched to 120 and 180% elongation were originally only 0.40 cm across before elongation and were therefore smaller than the four platinum contact wires. It was only possible to carry out parallel-conductivity measurements on these samples.

2.4. DSC measurements

For the DSC results, samples of PANi·AMPSA$_{0.3}$, PANi·AMPSA$_{0.6}$ and PANi·AMPSA$_{1.0}$ films were heated between 208 and 523 K at a rate of 10 K min^{-1}, under a nitrogen atmosphere, using a Perkin–Elmer 7 Series thermal analysis system.

3. Results

3.1. Conductivity/temperature results for unoriented films

Graphs of conductivity versus temperature for PANi·AMPSA$_x$, where $0.3 < x < 1.0$, are shown in figure 2. The curves show some similarities to those previously observed for PANi·CSA$_x$ [4], with the differences summarized in table 1. Error bars have not been included in the graphs, as the systematic errors due to current, voltage and temperature measurements are smaller than the points. The larger systematic errors, arising mainly from measurements of the thickness and width of the films, are mentioned in the tables.

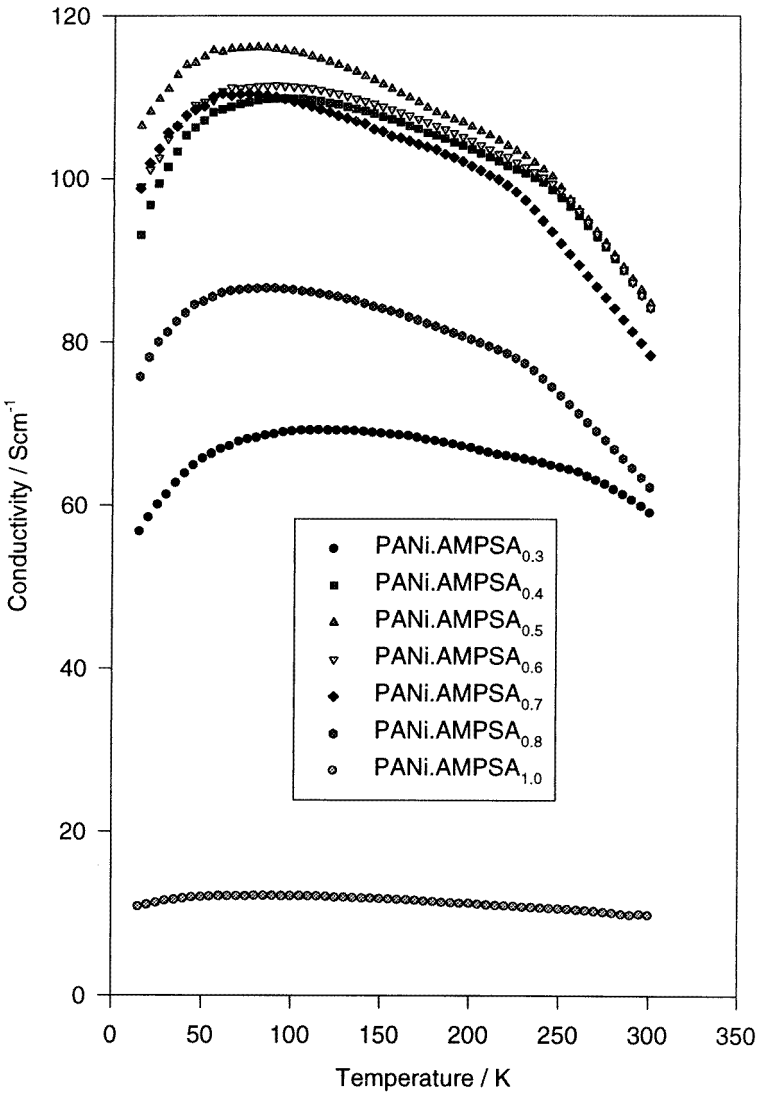

Figure 2. Graphs of conductivity versus temperature for unoriented solvent cast films of PANi·AMPSA$_x$, where $0.3 < x < 1.0$. Systematic errors are mentioned in table 1. The errors due to current, voltage and temperature measurements are too small to show.

Although the conductivity values for PANi·AMPSA$_x$ are lower than those for PANi·CSA$_x$, the temperatures at which maximum conductivity occurs are also lower. In addition, the ratio of $\sigma_{15\,K}/\sigma_{300\,K}$ for PANi·AMPSA$_x$ is greater than $\sigma_{10\,K}/\sigma_{300\,K}$ for PANi·CSA$_x$. These three observations hold for all values of x in the range $0.3 < x < 1.0$.

The maximum conductivity and lowest 'turnover' temperature for CSA-protonated polyaniline occurred when there was sufficient acid to protonate 60% of the nitrogens. It is not known whether all of the nitrogens were protonated, but there was a marked difference in conductivity, turnover temperature and crystallinity at 60% CSA from that at 50 or 70%. With AMPSA, the maximum conductivity and lowest turnover temperature occur with 50%

Table 1. Values for the peak conductivity, σ; the temperature at which the peak conductivity occurs; and ratios of $\sigma_{10\,K}/\sigma_{300\,K}$ for PANi·CSA$_x$ and $\sigma_{15\,K}/\sigma_{300\,K}$ for PANi·AMPSA$_x$. The peak-conductivity errors were estimated at ±10%, and the peak-conductivity temperature error at ±5 K.

	Peak conductivity, σ (S cm^{-1})		Temperature of peak σ (K)		$\sigma_{10\,K}/\sigma_{300\,K}$	$\sigma_{15\,K}/\sigma_{300\,K}$
Doping level (%)	CSA	AMPSA	CSA	AMPSA	CSA	AMPSA
30	90	69	270	115	0.13	0.96
40	160	110	225	95	0.44	1.10
50	178	116	190	75	0.67	1.26
60	268	111	135	85	0.94	1.18
70	184	110	184	80	0.75	1.26
80	—	87	—	85	—	1.22
90	121	—	185	—	0.71	—
100	—	12	—	85	—	1.11

Table 2. Heterogeneous model fitting parameters for PANi·AMPSA$_x$ data from figure 2.

AMPSA (%)	A (10^{-5} cm K^{-1})	B (10^{-3} cm)	T_0 (K)	T_1 (K)
30	1.63	10.0	37.3	53.1
40	1.10	6.80	21.5	34.1
50	1.35	5.85	36.9	66.6
60	1.20	6.34	31.4	54.9
70	1.28	6.72	21.5	40.6
80	1.79	7.70	36.9	57.0
100	12.9	54.7	37.6	60.6
PANi·CSA$_{0.5}$ †	0.66	0.93	519	332

† Data included for comparison from reference [4].

AMPSA, although the difference between this value and the ones for 40, 60 and 70% is small enough to be within experimental error. At present, it is not known whether all of the AMPSA is indeed protonating the polyaniline, especially with protonation levels greater than 50%. UV photoelectron spectroscopy techniques are currently being employed to study the bonding in these systems, and it is expected that these results will provide further clues to the precise interplay of the different chemical groups in the polymer films.

A major difference observed in the transport data for this new system is the presence of an additional transition point between 240 and 260 K, depending upon the sample, where the negative temperature coefficient of conductivity increases with increasing temperature. If the curves in figure 2 are normalized, the slopes of the graphs above 260 K are approximately equal, indicating that the transport mechanism as well as the transition point itself are independent of doping in films of PANi·AMPSA$_x$, where $0.4 < x < 0.8$. The high-temperature feature is not observed in films of PANi·CSA$_x$. This new phenomenon is discussed further in section 4.

To determine whether the same general transport mechanisms as were used previously for PANi·CSA$_x$ also hold for PANi·AMPSA$_x$, the heterogeneous model, as described previously [4], has been used to fit these new data. This took the form

$$1/\sigma = AT + B[\exp(-T_0/(T_1 + T))]^{-1}$$

where A and B are fitting parameters; with B representing the maximum resistivity at

$T = 0$ K, and T_1 and T_0 are characteristic temperatures used in the fluctuation-induced tunnelling (FIT) model [4]. T_0 is the temperature at which there is a significant contribution to conductivity from the FIT process and T_1 is the effective barrier height for regions between the metallic 'islands'.

The new data were fitted between 15 and 240 K, the temperature region in which the two systems are similar. The added complexity of the high-temperature transition in the AMPSA-protonated samples does not then need to be considered. Very acceptable fits are obtained for all protonation levels using this simple model, as shown in table 2. To model the full temperature range and include the high-temperature transition is more difficult. No combination of terms, including (for example) multiple-tunnelling contributions or phonon effects [12], can be used to model the entire temperature range. Hence, it is assumed that a phase transition occurs at 240–260 K, which gives rise to a marked discontinuity in transport properties.

3.2. DSC results for a film of PANi·AMPSA$_x$.

The DSC results for PANi·AMPSA$_{0.6}$ between 208 and 283 K are shown in figure 3. This shows an endothermic transition of magnitude 0.30 J g^{-1} K^{-1}, centred at 240 K. Above 280 K, the DSC trace is featureless, and the gentle rise indicative of a plasticized system. This would explain the ability of this material to be drawn at room temperature, unlike PANi·CSA$_{0.5}$, which could only be drawn at 420 K or higher [13].

A similar feature was seen in the DSC for a film of PANi·AMPSA$_{1.0}$. This showed a transition of magnitude 0.38 J g^{-1} K^{-1} centred at 254 K. A film of PANi·AMPSA$_{0.3}$ showed no observable transition. This may indicate that the transition is dependent upon the amount of AMPSA, which would suggest that the AMPSA is behaving like a side chain attached to the main polymer backbone through ionic bonds (and probably hydrogen bonding, in a manner similar to that found for PANi·CSA$_{0.5}$ [14]). This will allow subsequent motion of the polyaniline backbone as well, as is the case for *N*-alkyl-substituted PANi [15].

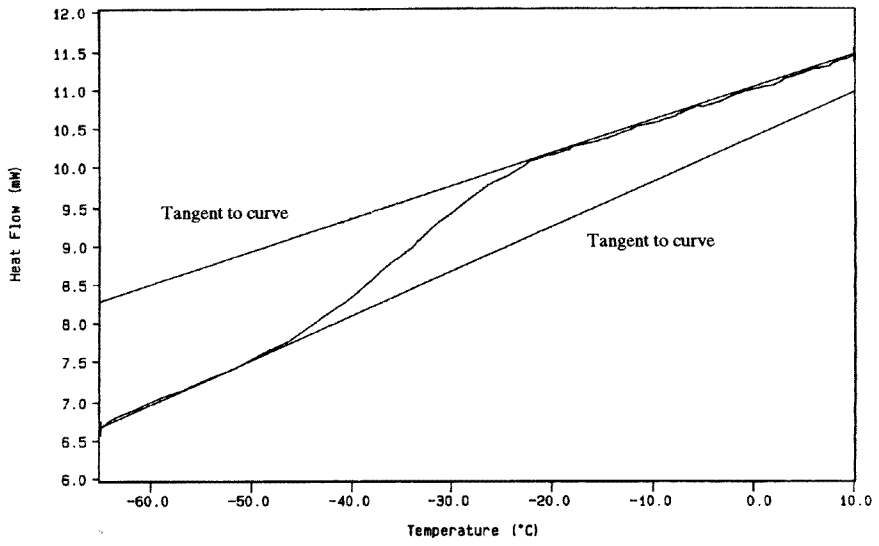

Figure 3. DSC for a film of PANi·AMPSA$_{0.6}$ between −65 and +10 °C.

3.3. Orientation and conductivity/temperature measurements on PANi·AMPSA$_{0.6}$

A dumb-bell-shaped film of PANi·AMPSA$_{0.6}$, with a surface area measuring 2.00×4.00 cm over the parallel portion, had a room temperature conductivity of 210 ± 20 S cm^{-1}. (It is thought that the conductivity is somewhat higher than that of the unstretched films in figure 2 due to the slower drying rate, which may have given more or bigger crystalline 'islands', resulting in higher conductivity.) After heating at 363 K and stretching to 150% of the original length, under an applied stress of 16.0 N, the room temperature conductivity along

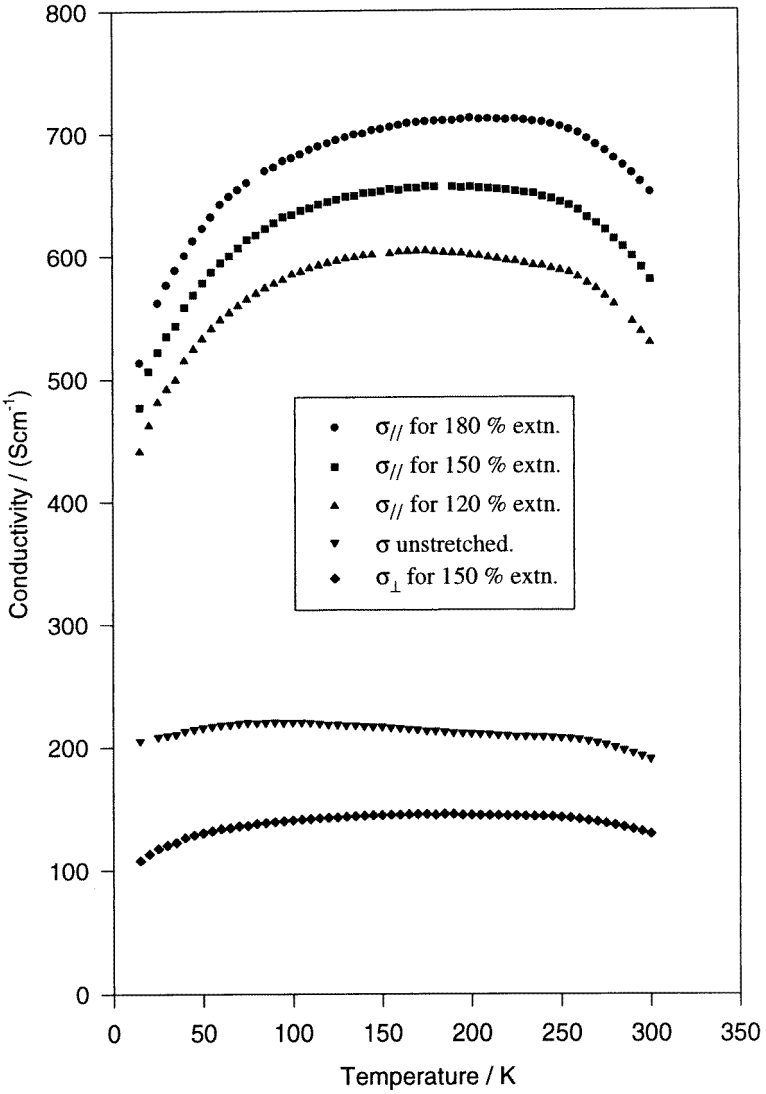

Figure 4. Graphs of conductivity versus temperature for stretched films of PANi·AMPSA$_{0.6}$. The systematic errors are mentioned in table 3. The errors due to current, voltage and temperature measurements are too small to show. Random errors due to electrical interference have been removed from the graphs.

the stretch direction ($\sigma_{\parallel}$) now measured 580 ± 40 S cm^{-1}. The conductivity perpendicular to the stretch direction ($\sigma_{\perp}$) measured 125 ± 10 S cm^{-1}. The electrical anisotropy measured 4.6 ± 0.6. The film thickness decreased from 0.0080 to 0.0046 ± 0.0002 cm and the width from 2.00 to 1.33 ± 0.01 cm. Further films, measuring 2.50×0.40 cm, were stretched to 120% and 180% of their original length to give room temperature conductivities ($\sigma_{\parallel}$) of 500 ± 35 and 670 ± 55 S cm^{-1} (thicknesses = 0.0048 and 0.0043 ± 0.0002 cm respectively). Gold electrodes were evaporated onto the films which were subsequently placed inside a cryostat before removing the air with a turbomolecular pump. The temperature was lowered to 15 K then increased to 300 K, with conductivity measurements taken every 5 K, as shown in figure 4. The results for these films are summarized in table 3.

Table 3. Conductivity/temperature results for stretched films of PANi·AMPSA$_{0.6}$. The systematic errors are shown in the table.

Percentage elongation	Peak conductivity, σ (S cm^{-1})	Temperature of peak σ (K)	$\sigma_{15\,K}/\sigma_{300\,K}$
0	220 ± 20	90 ± 5	1.08
120	600 ± 40	180 ± 5	0.83
150 (perpendicular)	145 ± 10	195 ± 5	0.83
150 (parallel)	655 ± 50	195 ± 5	0.82
180	710 ± 60	215 ± 5	0.79

It is clear from these results that, as the films are stretched, the conductivity along the stretch direction increases while that perpendicular to the stretch direction decreases, compared to those for an isotropic, unstretched film. In addition, the temperature at which peak conductivity occurs also increases, while the ratio of the conductivities at 15 K and 300 K decreases. As the percentage elongation increases, the negative temperature coefficient of conductivity decreases. The temperature dependences of the parallel- and perpendicular-conductivity components are similar and there is a constant anisotropy throughout the measured temperature range. These results are very similar to earlier results for cryopumped films of PANi·CSA$_{0.6}$ [16] which increased in conductivity from 268 to 583 S cm^{-1} on stretching by 100% (118% conductivity increase), while the temperature at which the maximum conductivity occurred rose from 135 to 215 K—an increase of 80 K.

The second transition at $\sim$250 K is also preserved, and does not appear to be dependent upon the degree of orientation. If this intramolecular effect is due to motion in the AMPSA anions, then the degree of orientation does not seem to affect this motion to any great extent.

To achieve further understanding of the orientation process, a second experiment was carried out after it was found that it was possible to cold draw AMPSA-protonated films to some degree. A dumb-bell-shaped film of PANi·AMPSA$_{0.6}$, with a cross sectional area measuring 0.40×0.015 cm over the parallel portion, had a room temperature conductivity of 170 ± 15 S cm^{-1}. After stretching to 100% of the original length at room temperature, under an applied stress of 5.5 N, the conductivity along the stretch direction measured 340 ± 40 S cm^{-1}. The film was still slightly elastic at this point, so it was heated to 383 K for 10 minutes under 5.5 N tension. The conductivity now measured 410 ± 40 S cm^{-1}. After a further 50 minutes of heating under stress, the conductivity measured 460 ± 40 S cm^{-1}. Further heating caused no further increase in conductivity. This contrasts with the case for samples of PANi·CSA$_{0.6}$, which had to be heated to 423 K before substantial orientation occurred [13]. Since residual DCA solvent will be removed fairly rapidly upon heating, it is believed that the AMPSA side-chain motion also allows the PANi chains to orient slowly

during the heating period under the action of applied stress, i.e. a form of annealing. We have found previously that any kind of annealing of CSA-protonated films is detrimental to their conductivity and mechanical strength.

4. Discussion

Transport data for PANi·AMPSA$_x$ over the range of 15–240 K are consistent with the results found previously for PANi·CSA$_x$, both in terms of temperature dependence and dependence upon the protonation level. As before, fitting the data to a heterogeneous model works well, although few trends are seen in the fitting parameters as a function of the protonation level. PANi·AMPSA$_{0.5}$ yields the lowest value for the B-coefficient, i.e. the resistivity at $T = 0$ K, and also has the highest conductivity (50% protonation may be expected to give the optimum conductivity if the polyaniline is in the emeraldine oxidation state). Generally speaking, the fitting does reveal that AMPSA produces lower hopping barriers than CSA (the last row in table 3), and the low-temperature turnover in the temperature dependence of the conductivity occurs at lower temperatures (table 1). This is thought to be due to the comparative geometrical structures of AMPSA and CSA. The former is essentially a branched but flexible structure, whilst the latter is more spherical, and likely to be a more rigid molecule (figure 1). It is assumed that the PANi·AMPSA$_x$ chains can pack together more closely, giving rise to smaller interchain distances, and hence lower barriers for carriers to surmount in hopping between chains (in the amorphous regions). This should be confirmed by x-ray studies to be undertaken in the near future.

The structure of the AMPSA anion also leads on to an understanding of the transition which occurs at $\simeq$240–260 K, which is not seen with CSA. DSC results show an endothermic transition occurring at 240–254 K, the magnitude of which is dependent upon the amount of AMPSA. This has been ascribed to increased motion in the AMPSA anions above this transition temperature. When this occurs, in what are essentially side chains, the polyaniline backbone will be able to move more readily, giving rise to increased intrachain phonon backscattering of carriers. This behaviour agrees well with the predictions of Kivelson and Heeger [17]. Above this transition temperature, the heterogeneous model cannot be used to describe charge transport. This high-temperature transition has been observed at the same temperature in oriented films as well, regardless of the degree of orientation. In addition, for PANi·AMPSA$_{0.3}$, only a weak transition at 260 K is observed in the transport data and none in the DSC trace. This gives clear evidence that the transitions around 250 K, in both the temperature dependence of the conductivity and the DSC trace, are caused by changes in the degree of motion in the AMPSA anions.

Orientation of PANi·AMPSA$_{0.6}$ films has been shown to occur, with similar results obtained to those previously demonstrated for PANi·CSA$_{0.5}$ [15]. AMPSA allows the possibility of cold drawing under stress, as well as elongation at elevated temperatures. Respectable conductivity increases along the stretch direction can be produced. The temperature-dependent conductivities of such oriented films show the same general form, both parallel and perpendicular to the stretch direction. In all cases, both the low-temperature localization turnover and the high-temperature transition due to side-chain motion are seen, as for the unstretched films. However, the low-temperature turnover point moves to higher temperatures, and the temperature dependence becomes weaker, with increasing elongation of the film. It has been shown previously that PANi·CSA$_{0.5}$ consists of crystalline regions in an amorphous matrix [19], most probably in the form of a switchboard lamellae structure. The metallic conductivity contribution scales proportionally to the degree of crystallinity. Therefore, it is assumed that metallic conduction occurs within these crystalline regions.

As the films are stretched, alignment of both the crystalline and amorphous regions takes place [18], leading to an increase in the conductivity. As the distance between crystallites increases due to stretching, the metallic response of the bulk polymer is reduced, leading to the increase in the temperature at which the maximum conductivity occurs. The presence of metallic carriers can still be detected in stretched films by reflectivity measurements. Determination of the plasma frequency showed that stretched films were more metallic, i.e. the plasma frequency shifted to a higher energy with film elongation [20]. Attempts to fit the conductivity data from stretched films of PANi·$AMPSA_{0.6}$ with the heterogeneous model were inconclusive.

The low-temperature turnover has been ascribed previously to the freezing out of the cooperative phenylene ring flipping mode [21] in HCl-protonated PANi [22] and CSA-protonated PANi [13], which leads to a localization of charge carriers. As films of PANi·$AMPSA_{0.6}$ are stretched, the amorphous regions become more ordered [18]. It is assumed that the polyaniline chains become more densely packed, making cooperative ring flips more difficult. More thermal excitation is required to induce ring flipping so that carrier transport will be more strongly temperature dependent.

5. Summary

Polyaniline has been cast into conductive films using 2-acrylamido-2-methyl-1-propane-sulphonic acid (AMPSA) as both the protonating acid and the solvating group, and dichloroacetic acid (DCA) as the solvent. The optimum conductivity is obtained when about 50% of the nitrogens in polyaniline are protonated, although the conductivity does not show much variation with protonation levels of between 40 and 70%. The conductivities are lower than those observed in polyaniline protonated with CSA and using m-cresol as a solvent, but the temperature at which the transition between non-metallic and metallic behaviour occurs is typically some 50–150 K lower for PANi·$AMPSA_x$ compared to PANi·CSA_x, where x is between 0.3 and 1.0.

The curves for the temperature dependence of the conductivity for PANi·$AMPSA_x$ show an additional feature between 240 and 260 K, where the conductivity becomes more temperature dependent. A DSC run for a sample of PANi·$AMPSA_{0.6}$ showed an endothermic transition of magnitude 0.30 J g^{-1} K^{-1} centred at 240 K, which has been ascribed to increased motion in the AMPSA side chains. This motion will allow increased movement in the PANi backbone and hence greater interchain phonon backscattering of charge carriers. This is in agreement with the predictions of Kivelson and Heeger on the nature of intrinsic conduction mechanisms in conjugated polymers [17]. The thermal transition comes about due to the comparatively flexible nature of the AMPSA molecule compared to the relatively spherical and rigid CSA, and is therefore not seen in films of PANi·CSA_x.

The transport data obtained below 240 K may be described adequately by employing the heterogeneous model used previously to model the PANi·CSA_x system. With PANi·$AMPSA_x$, the hopping barriers are lower than in the case of PANi·CSA_x. This may be understood once more in terms of the structure of the AMPSA anion, which will allow the PANi chains to pack together more closely than CSA anions. Interchain hopping will therefore require less energy.

The solvent-cast films may be uniaxially oriented under tension at room temperature or above. Stretching a film of PANi·$AMPSA_{0.6}$ by 180% at 363 K has given a maximum room temperature conductivity of 670 ± 55 S cm^{-1} along the stretch direction, compared to a maximum unstretched room temperature conductivity of 210 ± 20 S cm^{-1}. After stretching, the turnover temperature at which the transition from non-metallic to metallic

behaviour occurs is higher, and is dependent upon the degree of orientation. The film stretched to 150% elongation showed constant anisotropy throughout the temperature range. The increase in transition temperature is thought to be due to a hindering of intrachain cooperative phenylene ring flipping in aligned polymer films.

The high-temperature transition point at 240 K is unaffected by the orientation process, consistent with the hypothesis that it is caused by increased motion in the side chains. Intriguingly, as the bulk conductivity rises due to increased orientation of both the crystalline and amorphous regions in the film, the temperature dependency of the conduction mechanism weakens. This is thought to be due to the increased separation of the crystalline, metallic regions within the bulk of the films.

This new 'metallic' PANi system indicates how molecular dynamics impinges upon charge-carrier dynamics. By careful choice of counter-ion geometry, some control of the charge-transport mechanism may be achieved.

Acknowledgments

The authors would like to thank BICC and Paul Thacker for the DSC runs, and DERA for their funding for and collaboration in this work.

References

[1] Cao Y, Smith P and Heeger A J 1992 *Synth. Met.* **48** 91–7
[2] Wang Y Z, Joo J, Hsu C-H and Epstein A J 1995 *Synth. Met.* **68** 207–11
[3] Menon R, Yoon C O, Moses D and Heeger A J 1993 *Phys. Rev.* B **48** 17 685–94
[4] Holland E R, Pomfret S J, Adams P N and Monkman A P 1996 *J. Phys.: Condens. Matter* **8** 2991–3002
[5] Abell L, Pomfret S J, Adams P N, Middleton A C and Monkman A P 1997 *Synth. Met.* **84** 803–4
[6] Cao Y, Qiu J and Smith P 1995 *Synth. Met.* **69** 187–90
[7] Cao Y and Smith P 1995 *Synth. Met.* **69** 191–2
[8] Carter S A, Angelopoulos M, Korg S, Brock P J and Scott J C 1997 *Appl. Phys. Lett.* **70** 2067–9
[9] Pomfret S J, Adams P N, Comfort N and Monkman A P 1998 *Adv. Mater.* at press
[10] Adams P N, Laughlin P J, Monkman A P and Kenwright A M 1996 *Polymer* **37** 3411–7
[11] Adams P N and Monkman A P 1997 *UK Patent No* 2287030
[12] Kaiser A B and Graham S C 1990 *Synth. Met.* **36** 367–80
[13] Abell L, Pomfret S J, Adams P N and Monkman A P 1997 *Synth. Met.* **84** 127–8
[14] Ikkala O T, Pietila L, Ahjopalo L, Osterholm H and Passiniemi P J 1995 *J. Chem. Phys.* **22** 9855–63
[15] Zheng W-Y, Levon K, Laakso J and Osterholm J-E 1994 *Macromolecules* **27** 7754–68
[16] Holland E R, Pomfret S J, Adams P N, Abell L and Monkman A P 1997 *Synth. Met.* **84** 777–8
[17] Kivelson S and Heeger A J 1989 *Synth. Met.* **22** 371–82
[18] Abell L, Adams P N and Monkman A P 1996 *Polym. Commun.* **37** 5927–31
[19] Abell L, Devasagayam P, Adams P N and Monkman A P 1997 *Proc. SPE* **1414** 784–8
[20] Kohlman R S, Tanner D B, Ihas G G, Min Y G, MacDiarmid A G and Epstein A J 1997 *Synth. Met.* **84** 709–14
[21] Monkman A P, Adams P N, Milton A, Scully M and Pomfret S 1993 *Mol. Cryst. Liq. Cryst.* **236** 189–97
[22] Milton A and Monkman A P 1993 *J. Phys. D: Appl. Phys.* **26** 1468–74